

Unexpected Structures of Aluminum Oxide Clusters in the Gas Phase**

Marek Sierka,* Jens Döbler, Joachim Sauer, Gabriele Santambrogio, Mathias Brümmer, Ludger Wöste, Ewald Janssens, Gerard Meijer, and Knut R. Asmis*

Solid aluminum oxide (alumina) exists in many polymorphs,^[1] the most stable of which is α - Al_2O_3 (corundum). The structure of corundum consists of a hexagonal close packing of oxide ions in which the octahedral interstices are symmetrically occupied by aluminum cations. In contrast, in metastable alumina phases, such as γ - Al_2O_3 and δ - Al_2O_3 , a fraction of the aluminum ions occupy tetrahedral interstices.^[2] Ultrathin films of alumina contain tetrahedrally and square pyramidally (fivefold) coordinated aluminum sites.^[3] The variety of structures adopted under different conditions indicates the inherent flexibility of systems with the stoichiometry Al_2O_3 . Herein, we investigate the structural changes that occur on going from the bulk solid to small molecular clusters of composition $(\text{Al}_2\text{O}_3)_4$. Alumina structures of reduced dimensionality, such as small particles or thin films, are of interest in astrophysics^[4] and atmospheric chemistry,^[5] as well as in nanostructured ceramic materials, solid catalysts, and supports for catalysts.^[3,6,7] Model systems such as alumina clusters, mixed-metal oxide clusters,^[8] and oxide clusters supported on oxide films^[7] can help in the understanding of more complex supported catalysts.

Recent advances in vibrational spectroscopy have contributed significantly to the structural characterization of mass-selected metal oxide clusters and cluster ions.^[9–12] Infrared (IR) resonance-enhanced multiple-photon ionization (REMPI) spectra for small neutral aluminum oxide clusters^[9,13,14] show two absorption bands assigned to “lattice-like” structures that resemble γ - Al_2O_3 , rather than α - Al_2O_3 .

Cluster ionization, cluster dissociation, and cluster ionization followed by dissociation are all feasible channels, which have comparable energies in these alumina systems. This situation complicates the interpretation of the experimental IR-REMPI spectra and makes the assignment to individual cluster structures difficult. Previously, structural models of oxide clusters have been proposed on the basis of chemical intuition, but only in a few cases have definitive structure assignments been made.^[12,15]

In this study, we show that the most stable isomers of the $[(\text{Al}_2\text{O}_3)_4]^+$ and $(\text{Al}_2\text{O}_3)_4$ clusters exhibit new structural features that are not found in any known solid polymorph of Al_2O_3 . Their structures were determined through the combination of experiment and density functional theory (DFT), with the implementation of a genetic algorithm (GA) as a global optimization technique.^[16] We further show that, contrary to general expectations, the structures of neutral and cationic clusters are substantially different. The IR multiple-photon dissociation (MPD) spectrum collected for $[(\text{Al}_2\text{O}_3)_4]^+$ confirms the structure predicted by the GA. In contrast, the experimental spectrum showed little similarity to that simulated for the DFT-optimized structure of cluster fragment of the α - Al_2O_3 structure (Figure 1a). In many previous studies, this compact isomer with D_{3d} symmetry was assumed to be the global minimum for $(\text{Al}_2\text{O}_3)_4$, and this isomer was also used as a model for the bulk and surface of α - Al_2O_3 .^[17] In fact, it was the disagreement with experiment that triggered our search for a new cluster structure.

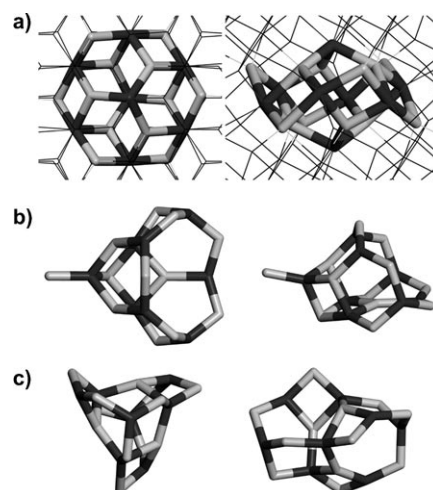


Figure 1. Optimized structures of the aluminum oxide clusters. a) The α - $(\text{Al}_2\text{O}_3)_4$ cluster superimposed with the corundum lattice (thin lines). b) The global minimum of the cationic $[(\text{Al}_2\text{O}_3)_4]^+$ cluster. c) The global minimum of the neutral $(\text{Al}_2\text{O}_3)_4$ cluster. Al black, O gray.

[*] Dr. M. Sierka, Dr. J. Döbler, Prof. Dr. J. Sauer
Institut für Chemie, Humboldt-Universität zu Berlin
Unter den Linden 6, 10099 Berlin (Germany)
Fax: (+49) 30-2093-7136
E-mail: marek.sierka@chemie.hu-berlin.de

Prof. Dr. G. Meijer, Dr. K. R. Asmis
Fritz-Haber-Institut der Max-Planck-Gesellschaft
Faradayweg 4–6, 14195 Berlin (Germany)
Fax: (+49) 30-8413-5603
E-mail: asmis@fhi-berlin.mpg.de

Dipl.-Phys. G. Santambrogio, Dr. M. Brümmer, Prof. Dr. L. Wöste
Institut für Experimentalphysik, Freie Universität Berlin
Arnimallee 14, 14195 Berlin (Germany)

Dr. E. Janssens
Laboratorium voor Vaste-Stoffysica en Magnetisme
Katholieke Universiteit Leuven
Celestijnenlaan 200D, 3001 Leuven (Belgium)

[**] The authors thank the Fonds der Chemischen Industrie and the Deutsche Forschungsgemeinschaft (SFB 546) for financial support, the Stichting voor Fundamenteel Onderzoek der Materie (FOM) for beamtime on FELIX, and the technical staff of FELIX for their assistance with the experiments.

The topology of the $(\text{Al}_2\text{O}_3)_4$ clusters (Figure 1) can be characterized on the basis of n -membered (nm) rings consisting of alternating aluminum and oxygen atoms. The compact structure of the neutral $(\text{Al}_2\text{O}_3)_4$ corundum fragment (Figure 1a), denoted as α - $(\text{Al}_2\text{O}_3)_4$, consists of 6m and 4m rings only. The cluster contains six fourfold- and two threefold-coordinated aluminum atoms, as well as six twofold- and six threefold-coordinated oxygen atoms; the Al–O bond lengths are 1.71–1.91 Å. The symmetry of the cationic $[(\text{Al}_2\text{O}_3)_4]^+$ cluster is lowered to C_s through a first-order Jahn–Teller effect. However, the distortion of the structure is relatively small, and the main structural features remain unchanged. The global optimization of the cationic $[(\text{Al}_2\text{O}_3)_4]^+$ cluster yields a C_s -symmetric structure with an “arrowhead” shape (Figure 1b). This structure is 125 (B3LYP) or 122 kJ mol^{-1} (MP2) more stable than the α - $[(\text{Al}_2\text{O}_3)_4]^+$ cluster. The base of the arrowhead is formed by five 6m rings, which are fused such that a 10m ring is formed at the bottom of the arrowhead and a 6m ring is formed at the top. An additional oxygen atom above the top 6m ring connects three 4m rings into a cube fragment. A final oxygen atom is coordinated to the topmost aluminum vertex of the cube fragment, forming the tip of the arrowhead. The cluster contains three fourfold- and five threefold-coordinated aluminum atoms, as well as seven twofold-, four threefold-, and one onefold-coordinated oxygen atom. The Al–O bond lengths range from 1.69–1.87 Å; those in the 10m ring at the bottom of the arrowhead are the shortest (1.69–1.73 Å). The singly coordinated oxygen atom at the tip of the arrowhead is bonded at an Al–O distance of 1.74 Å.

In Figure 2, the experimental IR-MPD spectrum (a) is compared to the calculated linear IR absorption spectra for the global-minimum $[(\text{Al}_2\text{O}_3)_4]^+$ cluster (b) and the α - $[(\text{Al}_2\text{O}_3)_4]^+$ cluster (c). The calculated spectrum of the corundum-derived structure has little similarity with the experimental spectrum, whereas the spectrum of the global-minimum structure shows excellent agreement. All the observed vibrational bands are reproduced, albeit with different intensities. Deviations between IR-MPD and calculated IR absorption spectra are not unexpected.^[10,18] A characteristic vibrational band occurs near 1030 cm^{-1} in the experimental spectrum. As bands with such an unusually high frequency are unknown for bulk Al_2O_3 , it could be inferred that this band arises from the stretching vibration of a terminal Al–O bond. However, analysis of the vibrational modes of the global-minimum $[(\text{Al}_2\text{O}_3)_4]^+$ cluster demonstrates that this fingerprint vibration is an out-of-phase coupling of asymmetric Al–O–Al stretching vibrations (Figure 3a). The stretching vibration of the terminal Al–O bond is located near 870 cm^{-1} . Out of dozens of calculated $[(\text{Al}_2\text{O}_3)_4]^+$ structures, only the global-minimum structure produces the 1030 cm^{-1} vibration.

The question arises as to what drives the $[(\text{Al}_2\text{O}_3)_4]^+$ cluster to assume the unusual arrowhead shape with one singly coordinated oxygen atom. The answer is provided by the spin-density distribution (Figure 3b) and the differential electrostatic potential (Figure 3c) of the global-minimum structure, which show that the single unpaired electron and the positive charge are both localized at the singly coordinated oxygen atom. Thus, the terminal bond is formally an

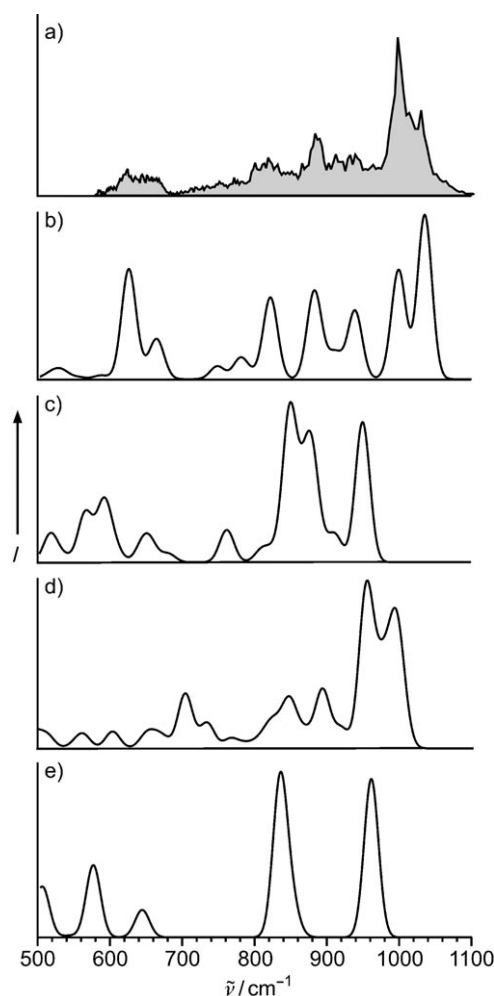


Figure 2. Comparison of a) the experimental IR-MPD spectrum ($[\text{Al}_8\text{O}_{11}]^+$ signal) of the $[(\text{Al}_2\text{O}_3)_4]^+$ cluster to the calculated linear IR absorption spectra of b) the global minimum of the cationic $[(\text{Al}_2\text{O}_3)_4]^+$ cluster, c) the cationic α - $[(\text{Al}_2\text{O}_3)_4]^+$ cluster, d) the global minimum of the neutral $(\text{Al}_2\text{O}_3)_4$ cluster, and e) the neutral α - $(\text{Al}_2\text{O}_3)_4$ cluster. For a better comparison, the calculated spectra in (b–e) were convoluted with Gaussian functions (full width at half maximum of ca. 24 cm^{-1}).

Al–O• single bond, which explains the unusually low frequency of the corresponding stretching vibration. We conclude that electrostatic interactions may be the driving force responsible for the arrowhead shape of the cluster, since a comparable localization of the positive charge is not possible in the α - $[(\text{Al}_2\text{O}_3)_4]^+$ cluster.

The good agreement between the experimental and calculated IR spectra for the global-minimum $[(\text{Al}_2\text{O}_3)_4]^+$ cluster provides confidence in our GA implementation and in the ability of the B3LYP method to properly describe Al_2O_3 structures. Therefore, we also performed a global minimization for the neutral $(\text{Al}_2\text{O}_3)_4$ cluster, for which experimental data cannot easily be obtained. The topology and the atomic positions of the global-minimum structure (Figure 1c) also differ substantially from those of the α - $(\text{Al}_2\text{O}_3)_4$ structure. The $(\text{Al}_2\text{O}_3)_4$ cluster consists of 8m, 6m, and 4m rings. The center of the cluster is formed by three 4m rings that are each linked to the two other 4m rings by one aluminum and one

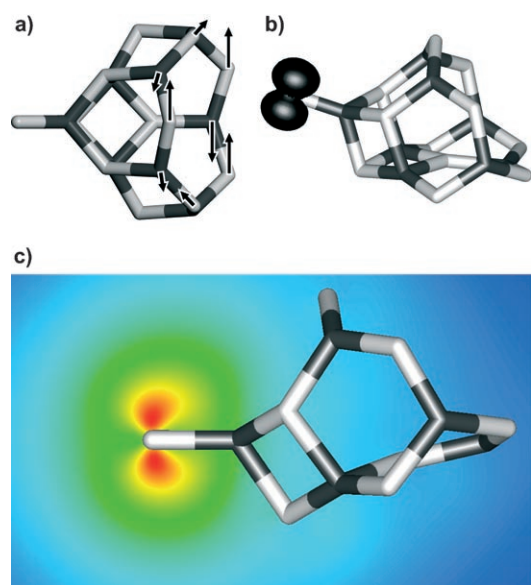


Figure 3. a) Schematic representation of the fingerprint vibrational mode at 1030 cm^{-1} of the global minimum of the $[(\text{Al}_2\text{O}_3)_4]^+$ cluster. b) The calculated spin density (black) of the $[(\text{Al}_2\text{O}_3)_4]^+$ cluster. c) The difference between the calculated electrostatic potentials of the neutral and cationic states of the global minimum of the $[(\text{Al}_2\text{O}_3)_4]^+$ cluster (blue to red with increasing negative potential). Al black, O gray.

oxygen vertex. Two additional threefold-coordinated aluminum atoms are connected via twofold-coordinated oxygen atoms to the aluminum vertices on opposite sides of the three 4m rings. The average coordination numbers of the aluminum and oxygen atoms are lower than those in the $\alpha\text{-(Al}_2\text{O}_3)_4$ fragment. There are three fourfold- and five threefold-coordinated aluminum atoms, as well as nine twofold- and three threefold-coordinated oxygen atoms. The Al–O bond lengths also span a slightly broader range of $1.70\text{--}1.94\text{ \AA}$. The calculated energy difference between the neutral global-minimum $(\text{Al}_2\text{O}_3)_4$ and $\alpha\text{-(Al}_2\text{O}_3)_4$ clusters is 47 (B3-LYP) or 20 kJ mol^{-1} (MP2). As a reference for future experiments, we present the calculated IR spectrum for the global-minimum $(\text{Al}_2\text{O}_3)_4$ cluster (Figure 2d), which is substantially different from that calculated for the $\alpha\text{-(Al}_2\text{O}_3)_4$ cluster (Figure 2e).

In summary, we have demonstrated that a corundum fragment is not the global minimum for the neutral $(\text{Al}_2\text{O}_3)_4$ cluster nor for the cationic $[(\text{Al}_2\text{O}_3)_4]^+$ cluster in the gas phase. The global-minimum structures of the neutral and cationic clusters have no features in common with any of the known bulk Al_2O_3 phases. The results of our calculations on the cluster cation are fully supported by the experimental IR-MPD spectra. Our results show that, in contrast to general belief, the charge of gas-phase oxide clusters has a dramatic effect on their structure: the structures of $(\text{Al}_2\text{O}_3)_4$ and $[(\text{Al}_2\text{O}_3)_4]^+$ are completely different.

Experimental Section

All calculations were performed using the TURBOMOLE program package.^[19] The global optimizations of the cluster structures were carried out at the DFT level with the B3LYP^[20] exchange-correlation

functional and split valence plus polarization (SVP) basis sets.^[21] We applied our own implementation of a GA after the original idea of Daeven and Ho.^[16c] The final structure optimizations and harmonic-frequency calculations were performed using the B3LYP functional and triple-zeta valence plus polarization (TZVP)^[21] basis sets for all atoms. Single-point MP2 calculations were performed for the DFT-optimized structures using the resolution of the identity approximation,^[22] and TZVP^[21] and auxiliary^[23] basis sets.

The cluster-generation experiments were carried out on a previously described tandem mass-spectrometer–ion-trap system.^[24] Aluminum oxide clusters were prepared by the pulsed-laser vaporization of an aluminum target in the presence of 1% oxygen in helium gas. The beam of positive ions was collimated and mass-selected by a quadrupole mass filter. Mass-selected cluster ions were accumulated and cooled in a linear radio-frequency ion trap held at 16 K. IR-MPD spectra were obtained by photoexcitation of the trapped cold ions with pulsed radiation from the free-electron laser for infrared experiments (FELIX) at the FOM Institute for Plasma Physics Rijnhuizen,^[25] and subsequent monitoring of the mass-selected $[\text{Al}_8\text{O}_{11}]^+$ ion yield (oxygen-atom loss channel). A FELIX root mean square (RMS) bandwidth of less than 0.3% of the central wavelength and pulse energies of up to 50 mJ were used.

Received: November 28, 2006

Published online: March 27, 2007

Keywords: cluster compounds · density functional calculations · genetic algorithms · IR photodissociation spectroscopy · structure elucidation

- [1] I. Levin, D. Brandon, *J. Am. Ceram. Soc.* **1998**, *81*, 1995–2012.
- [2] X. Krokidis, P. Raybaud, A.-E. Gobichon, B. Rebours, P. Euzen, H. Toulhoat, *J. Phys. Chem. B* **2001**, *105*, 5121–5130.
- [3] G. Kresse, M. Schmid, E. Napetschnig, M. Shishkin, L. Köhler, P. Varga, *Science* **2005**, *308*, 1440–1442.
- [4] T. Posch, F. Kerschbaum, H. Mutschke, D. Fabian, J. Dorschner, J. Horn, *Astron. Astrophys.* **1999**, *352*, 609–618.
- [5] a) K. M. Dill, R. A. Reed, V. S. Calia, R. J. Schulz, *J. Propul. Power* **1990**, *6*, 668–671; b) R. P. Turco, O. B. Toon, R. C. Whitten, R. J. Cicerone, *Nature* **1982**, *298*, 830–832.
- [6] G. E. Brown, Jr., V. E. Henrich, W. H. Casey, D. L. Clark, C. Eggleston, A. Felmy, D. W. Goodman, M. Grätzel, G. Maciel, M. I. McCarthy, K. H. Nealson, D. A. Sverjensky, M. F. Toney, J. M. Zachara, *Chem. Rev.* **1999**, *99*, 77–174.
- [7] N. Magg, J. B. Giorgi, T. Schroeder, M. Bäumer, H.-J. Freund, *J. Phys. Chem. B* **2002**, *106*, 8756–8761.
- [8] E. Janssens, G. Santambrogio, M. Brümmer, L. Wöste, P. Lievens, J. Sauer, G. Meijer, K. R. Asmis, *Phys. Rev. Lett.* **2006**, *96*, 233401.
- [9] G. von Helden, A. Kirilyuk, D. van Heijnsbergen, B. Sartakov, M. A. Duncan, G. Meijer, *Chem. Phys.* **2000**, *262*, 31–39.
- [10] G. von Helden, D. van Heijnsbergen, G. Meijer, *J. Phys. Chem. A* **2003**, *107*, 1671–1688.
- [11] K. R. Asmis, A. Fielicke, G. von Helden, G. Meijer in *The Chemical Physics of Solid Surfaces. Atomic Clusters: From Gas Phase to Deposited*, Vol. 12 (Ed.: P. Woodruff), Elsevier, **2007**, in press.
- [12] K. R. Asmis, J. Sauer, *Mass. Spectrom. Rev.* **2007**, in press.
- [13] D. van Heijnsbergen, K. Demyk, M. A. Duncan, G. Meijer, G. von Helden, *Phys. Chem. Chem. Phys.* **2003**, *5*, 2515–2519.
- [14] K. Demyk, D. van Heijnsbergen, G. von Helden, G. Meijer, *Astron. Astrophys.* **2004**, *420*, 547–552.
- [15] K. R. Asmis, G. Santambrogio, M. Brümmer, J. Sauer, *Angew. Chem.* **2005**, *117*, 3182–3185; *Angew. Chem. Int. Ed.* **2005**, *44*, 3122–3125.

- [16] Selected reviews and original contributions: a) R. L. Johnston, *Dalton Trans.* **2003**, 4193–4207; b) B. Hartke, *Angew. Chem.* **2002**, *114*, 1534–1554; *Angew. Chem. Int. Ed.* **2002**, *41*, 1468–1487; c) D. M. Deaven, K. M. Ho, *Phys. Rev. Lett.* **1995**, *75*, 288–291.
- [17] Selected contributions: a) E. M. Fernandez, R. Eglitis, G. Borstel, L. C. Balbás, *Phys. Status Solidi B* **2005**, *242*, 807–809; b) A. K. Gianotto, J. W. Rawlinson, K. C. Cossel, J. E. Olson, A. D. Appelhans, G. S. Groenewold, *J. Am. Chem. Soc.* **2004**, *126*, 8275–8283; c) M. Casarin, C. Maccato, A. Vittadini, *Inorg. Chem.* **2000**, *39*, 5232–5237; d) E. F. Sawilowsky, O. Meroueh, H. B. Schlegel, W. L. Hase, *J. Phys. Chem. A* **2000**, *104*, 4920–4927; e) J. M. Wittbrodt, W. L. Hase, H. B. Schlegel, *J. Phys. Chem. B* **1998**, *102*, 6539–6548.
- [18] J. Oomens, B. G. Sartakov, G. Meijer, G. von Helden, *Int. J. Mass Spectrom.* **2006**, *254*, 1–19.
- [19] a) R. Ahlrichs, M. Bär, M. Häser, H. Horn, C. Kölmel, *Chem. Phys. Lett.* **1989**, *162*, 165–169; b) O. Treutler, R. Ahlrichs, *J. Chem. Phys.* **1995**, *102*, 346–354.
- [20] a) A. D. Becke, *J. Chem. Phys.* **1993**, *98*, 5648–5652; b) C. Lee, W. Yang, R. G. Parr, *Phys. Rev. B* **1988**, *37*, 785–789.
- [21] F. Weigend, R. Ahlrichs, *Phys. Chem. Chem. Phys.* **2005**, *7*, 3297–3305.
- [22] F. Weigend, M. Häser, *Theor. Chem. Acc.* **1997**, *97*, 331–340.
- [23] a) F. Weigend, M. Häser, H. Patzelt, R. Ahlrichs, *Chem. Phys. Lett.* **1998**, *294*, 143–152; b) A. Hellweg, C. Hättig, S. Höfener, W. Klopper, *Theor. Chem. Acc.* **2007**, in press.
- [24] K. R. Asmis, M. Brümmer, C. Kaposta, G. Santambrogio, G. von Helden, G. Meijer, K. Rademann, L. Wöste, *Phys. Chem. Chem. Phys.* **2002**, *4*, 1101–1104.
- [25] D. Oeppts, A. F. G. van der Meer, P. W. van Amersfoort, *Infrared Phys. Technol.* **1995**, *36*, 297–308.